

$b \rightarrow s\gamma$ decay in the two Higgs doublet model with flavor changing neutral currents

T. M. Aliev ,

Physics Department, Girne American University
Girne , Mersin-10, Turkey

E. O. Iltan ^{*}

Physics Department, Middle East Technical University
Ankara, Turkey

Abstract

We study the $b \rightarrow s\gamma$ decay including the leading logarithmic QCD corrections in the two Higgs doublet model with flavor changing neutral currents at the tree level. Further, we find the constraints to the flavor changing parameters of the model, using the experimental results of $B \rightarrow X_s\gamma$ decay provided by the CLEO Collaboration.

^{*}E-mail address: eiltan@heraklit.physics.metu.edu.tr

1 Introduction

Rare B meson decays are one of the most promising research area in particle physics and lie on the focus of theoretical and experimental physicists. In the Standard Model (SM), they are induced by flavor changing neutral currents (FCNC) at loop level and therefore sensitive to the gauge structure of the theory. From the experimental point of view, they play an outstanding role in the precise determination of the fundamental parameters of SM, such as Cabibbo-Kobayashi-Maskawa (CKM) matrix elements, leptonic decay constants, etc. Furthermore, these decays provide a sensitive test to the new physics beyond the SM, such as two Higgs Doublet model (2HDM), Minimal Supersymmetric extension of the SM (MSSM) [1], etc. Among the rare B decays, $b \rightarrow s\gamma$ has received considerable interest since the branching ratios (Br) of the inclusive $B \rightarrow X_s\gamma$ [2] and exclusive $B \rightarrow K^*\gamma$ [3] have been already measured experimentally. Therefore, the $b \rightarrow s\gamma$ decay is under an extensive investigation in the framework of various extensions of the SM, in order to get information about the model parameters or improve the existing restrictions.

It is well known that the FCNC are forbidden at the tree level in the SM. This restriction is achieved in the extended model with the additional conditions. 2HDM is one of the simplest extensions of the SM, obtained by the addition of a new scalar $SU(2)$ doublet. The Yukawa lagrangian causes that the model possesses phenemologically dangerous FCNC's at the tree level. To protect the model from such terms, the ad hoc discrete symmetry [4] on the 2HDM scalar potential and the Yukawa interaction is proposed and there appears two different versions of the 2HDM depending on whether up and down quarks couple to the same or different scalar doublets. In model I, the up and down quarks get mass via vacuum expectation value (v.e.v.) of only one Higgs field. In model II, which coincides with the MSSM in the Higgs sector, the up and down quarks get mass via v.e.v. of the Higgs fields H_1 and H_2 respectively where $H_1(H_2)$ corresponds to first (second) Higgs doublet of 2HDM [5]. In the absence of the mentioned discrete symmetry, FCNC appears at the tree level and this model is called as model III in current literature [6, 7, 8]. A comprehensive phenemological analysis of the model III was done in series of works [6, 7, 9]. In particular, from a purely phenomenological point of view, low energy experiments involving $K^0 - \bar{K}^0$, $B^0 - \bar{B}^0$, $K_L \rightarrow \mu\bar{\mu}$ place strong constraints on the existence of tree level flavor changing (FC) transitions, existing in the model III.

In the present work, we examine the $b \rightarrow s\gamma$ decay in the model III with the addition of QCD corrections in the LLog approximation. Further, we obtain the constraints for the neutral couplings ξ_{Ntt}^U , ξ_{Nbb}^D and ξ_{Ntc}^U with the assumption that the couplings ξ_{Ncc}^U , $\xi_{Ns b}^D$ and $\xi_{Ns s}^D$ are

negligible compared to former ones (for the definition of $\xi_{N,ij}$ see section 2). Our predictions are based on the CLEO measurement $B \rightarrow X_s \gamma$ and lower bound for ξ_{bb}^D [6], which is estimated by using $R_b^{exp} = \Gamma(Z \rightarrow b\bar{b})/\Gamma(Z \rightarrow \text{hadrons})$ ratio.

The paper is organized as follows: In Section 2, we present the LLog QCD corrected Hamiltonian responsible for the $b \rightarrow s\gamma$ decay in the model III and discuss the effects of the additional *Left–Right* flipped operators to the decay rate. Section 3 is devoted to the constraint analysis, more precisely to the the ratios $\frac{\xi_{Ntt}^U}{\xi_{Nbb}^D}$, $\frac{\xi_{Ntc}^U}{\xi_{Nbb}^D}$ and their dependences on the QCD scale parameter μ , the charged Higgs boson mass, m_{H^\pm} , and our conclusions.

2 Leading logarithmic improved short-distance contributions in the model III for the decay $b \rightarrow s\gamma$

In this section we present the LLog QCD corrections to the $b \rightarrow s\gamma$ decay amplitude in the 2HDM (model III). Before the calculations, we would like to remind briefly the main features of the 2HDM. The Yukawa interaction for the general case is

$$\mathcal{L}_Y = \eta_{ij}^U \bar{Q}_{iL} \tilde{\phi}_1 U_{jR} + \eta_{ij}^D \bar{Q}_{iL} \phi_1 D_{jR} + \xi_{ij}^U \bar{Q}_{iL} \tilde{\phi}_2 U_{jR} + \xi_{ij}^D \bar{Q}_{iL} \phi_2 D_{jR} + h.c. \quad (1)$$

where L and R denote chiral projections $L(R) = 1/2(1 \mp \gamma_5)$, ϕ_i for $i = 1, 2$, are the two scalar doublets, $\eta_{ij}^{U,D}$ and $\xi_{ij}^{U,D}$ are the matrices of the Yukawa couplings. For convenience we choose ϕ_1 and ϕ_2 in the following basis:

$$\phi_1 = \frac{1}{\sqrt{2}} \left[\begin{pmatrix} 0 \\ v + H^0 \end{pmatrix} + \begin{pmatrix} \sqrt{2}\chi^+ \\ i\chi^0 \end{pmatrix} \right]; \phi_2 = \frac{1}{\sqrt{2}} \begin{pmatrix} \sqrt{2}H^+ \\ H_1 + iH_2 \end{pmatrix}, \quad (2)$$

where the vacuum expectation values are,

$$\langle \phi_1 \rangle = \frac{1}{\sqrt{2}} \begin{pmatrix} 0 \\ v \end{pmatrix}; \langle \phi_2 \rangle = 0. \quad (3)$$

This choice permits us to write the FC part of the interaction as

$$\mathcal{L}_{Y,FC} = \xi_{ij}^U \bar{Q}_{iL} \tilde{\phi}_2 U_{jR} + \xi_{ij}^D \bar{Q}_{iL} \phi_2 D_{jR} + h.c. , \quad (4)$$

with the following advantages:

- doublet ϕ_1 corresponds to the scalar doublet of the SM and H_0 to the SM Higgs field. This part of the Yukawa Lagrangian is responsible for the generation of the fermion masses with the couplings $\eta^{U,D}$.
- all new scalar fields belong to the ϕ_2 scalar doublet.

The couplings $\xi^{U,D}$ are the open window for the tree level FCNC's and can be expressed for the FC charged interactions as

$$\begin{aligned}\xi_{ch}^U &= \xi_{neutral} V_{CKM} , \\ \xi_{ch}^D &= V_{CKM} \xi_{neutral} ,\end{aligned}\tag{5}$$

where $\xi_{neutral}^{U,D}$ ¹ is defined by the expression

$$\xi_N^{U,D} = (V_L^{U,D})^{-1} \xi^{U,D} V_R^{U,D} .\tag{6}$$

Here the charged couplings appear as a linear combinations of neutral couplings multiplied by V_{CKM} matrix elements. This gives an important distinction between model III and model II (I).

After this preliminary remark, let us discuss the LLog QCD corrections to $b \rightarrow s\gamma$ decay in the 2HDM for the general case. The appropriate framework is that of an effective theory obtained by integrating out the heavy degrees of freedom, which are, in this context, t quark, W^\pm, H^\pm, H_1 , and H_2 bosons, where H^\pm denote charged, H_1 and H_2 denote neutral Higgs bosons. The LLog QCD corrections are done through matching the full theory with the effective low energy theory at the high scale $\mu = m_W$ and evaluating the Wilson coefficients from m_W down to the lower scale $\mu \sim O(m_b)$. Note that we choose the higher scale as $\mu = m_W$ since the evaluation from the scale $\mu = m_{H^\pm}$ to $\mu = m_W$ gives negligible contribution to the Wilson coefficients. Here we assume that the charged Higgs boson is heavy due to current experimental restrictions.

The effective Hamiltonian relevant for our process is

$$\mathcal{H}_{eff} = -4 \frac{G_F}{\sqrt{2}} V_{tb} V_{ts}^* \sum_i C_i(\mu) O_i(\mu) ,\tag{7}$$

where the O_i are operators given in eq. (8) and the C_i are Wilson coefficients renormalized at the scale μ . The coefficients are calculated perturbatively and expressed as functions of the heavy particle masses in the theory.

The operator basis depends on the model used and the conventional choice in the case of SM, 2HDM model II (I) and MSSM is

$$\begin{aligned}O_1 &= (\bar{s}_{L\alpha} \gamma_\mu c_{L\beta})(\bar{c}_{L\beta} \gamma^\mu b_{L\alpha}), \\ O_2 &= (\bar{s}_{L\alpha} \gamma_\mu c_{L\alpha})(\bar{c}_{L\beta} \gamma^\mu b_{L\beta}),\end{aligned}$$

¹In all next discussion we denote $\xi_{neutral}^{U,D}$ as $\xi_N^{U,D}$.

$$\begin{aligned}
O_3 &= (\bar{s}_{L\alpha} \gamma_\mu b_{L\alpha}) \sum_{q=u,d,s,c,b} (\bar{q}_{L\beta} \gamma^\mu q_{L\beta}), \\
O_4 &= (\bar{s}_{L\alpha} \gamma_\mu b_{L\beta}) \sum_{q=u,d,s,c,b} (\bar{q}_{L\beta} \gamma^\mu q_{L\alpha}), \\
O_5 &= (\bar{s}_{L\alpha} \gamma_\mu b_{L\alpha}) \sum_{q=u,d,s,c,b} (\bar{q}_{R\beta} \gamma^\mu q_{R\beta}), \\
O_6 &= (\bar{s}_{L\alpha} \gamma_\mu b_{L\beta}) \sum_{q=u,d,s,c,b} (\bar{q}_{R\beta} \gamma^\mu q_{R\alpha}), \\
O_7 &= \frac{e}{16\pi^2} \bar{s}_\alpha \sigma_{\mu\nu} (m_b R + m_s L) b_\alpha \mathcal{F}^{\mu\nu}, \\
O_8 &= \frac{g}{16\pi^2} \bar{s}_\alpha T_{\alpha\beta}^a \sigma_{\mu\nu} (m_b R + m_s L) b_\beta \mathcal{G}^{a\mu\nu},
\end{aligned} \tag{8}$$

where α and β are $SU(3)$ colour indices and $\mathcal{F}^{\mu\nu}$ and $\mathcal{G}^{\mu\nu}$ are the field strength tensors of the electromagnetic and strong interactions, respectively.

In our case, however, new operators with different chirality structures can arise since the general Yukawa lagrangian includes both L and R chiral interactions. The conventional operator set is extended first adding two new operators which are left-right analogues of O_1 and O_2 , namely

$$\begin{aligned}
O_9 &= (\bar{s}_{L\alpha} \gamma_\mu c_{L\beta}) (\bar{c}_{R\beta} \gamma^\mu b_{R\alpha}), \\
O_{10} &= (\bar{s}_{L\alpha} \gamma_\mu c_{L\alpha}) (\bar{c}_{R\beta} \gamma^\mu b_{R\beta}),
\end{aligned} \tag{9}$$

Further we need the second operator set $O'_1 - O'_{10}$ which are flipped chirality partners of $O_1 - O_{10}$:

$$\begin{aligned}
O'_1 &= (\bar{s}_{R\alpha} \gamma_\mu c_{R\beta}) (\bar{c}_{R\beta} \gamma^\mu b_{R\alpha}), \\
O'_2 &= (\bar{s}_{R\alpha} \gamma_\mu c_{R\alpha}) (\bar{c}_{R\beta} \gamma^\mu b_{R\beta}), \\
O'_3 &= (\bar{s}_{R\alpha} \gamma_\mu b_{R\alpha}) \sum_{q=u,d,s,c,b} (\bar{q}_{R\beta} \gamma^\mu q_{R\beta}), \\
O'_4 &= (\bar{s}_{R\alpha} \gamma_\mu b_{R\beta}) \sum_{q=u,d,s,c,b} (\bar{q}_{R\beta} \gamma^\mu q_{R\alpha}), \\
O'_5 &= (\bar{s}_{R\alpha} \gamma_\mu b_{R\alpha}) \sum_{q=u,d,s,c,b} (\bar{q}_{L\beta} \gamma^\mu q_{L\beta}), \\
O'_6 &= (\bar{s}_{R\alpha} \gamma_\mu b_{R\beta}) \sum_{q=u,d,s,c,b} (\bar{q}_{L\beta} \gamma^\mu q_{L\alpha}), \\
O'_7 &= \frac{e}{16\pi^2} \bar{s}_\alpha \sigma_{\mu\nu} (m_b L + m_s R) b_\alpha \mathcal{F}^{\mu\nu}, \\
O'_8 &= \frac{g}{16\pi^2} \bar{s}_\alpha T_{\alpha\beta}^a \sigma_{\mu\nu} (m_b L + m_s R) b_\beta \mathcal{G}^{a\mu\nu}, \\
O'_9 &= (\bar{s}_{R\alpha} \gamma_\mu c_{R\beta}) (\bar{c}_{L\beta} \gamma^\mu b_{L\alpha}), \\
O'_{10} &= (\bar{s}_{R\alpha} \gamma_\mu c_{R\alpha}) (\bar{c}_{L\beta} \gamma^\mu b_{L\beta}).
\end{aligned} \tag{10}$$

This extended basis is the same as the basis for $SU(2)_L \times SU(2)_R \times U(1)$ extensions of SM [10]. Note that in the SM, model II (I) 2HDM and the MSSM, the absence of O'_7 and O'_8 are a

consequence of assumption $m_s/m_b \sim 0$.

Now for the evaluation of Wilson coefficients, we need their initial values with standard matching computations. In the calculations, we take only the charged Higgs contributions into account and neglect the effects of the neutral Higgs bosons for the reasons, which we explain later.

Denoting the Wilson coefficients for the SM with $C_i^{SM}(m_W)$ and the additional charged Higgs contribution with $C_i^H(m_W)$, we have the initial values for the first set of operators (eqs. 8, 9) [13]

$$\begin{aligned} C_{1,3,\dots,6,9,10}^{SM}(m_W) &= 0, \\ C_2^{SM}(m_W) &= 1, \\ C_7^{SM}(m_W) &= \frac{3x^3 - 2x^2}{4(x-1)^4} \ln x + \frac{-8x^3 - 5x^2 + 7x}{24(x-1)^3}, \\ C_8^{SM}(m_W) &= -\frac{3x^2}{4(x-1)^4} \ln x + \frac{-x^3 + 5x^2 + 2x}{8(x-1)^3}, \end{aligned} \quad (11)$$

and

$$\begin{aligned} C_{1,\dots,6,9,10}^H(m_W) &= 0, \\ C_7^H(m_W) &= \frac{1}{m_t^2} (\bar{\xi}_{N,tt}^U + \bar{\xi}_{N,tc}^U \frac{V_{cs}^*}{V_{ts}^*}) (\bar{\xi}_{N,tt}^U + \bar{\xi}_{N,tc}^U \frac{V_{cb}}{V_{tb}}) F_1(y), \\ &+ \frac{1}{m_t m_b} (\bar{\xi}_{N,tt}^U + \bar{\xi}_{N,tc}^U \frac{V_{cs}^*}{V_{ts}^*}) (\bar{\xi}_{N,bb}^D + \bar{\xi}_{N,sb}^D \frac{V_{ts}}{V_{tb}}) F_2(y), \\ C_8^H(m_W) &= \frac{1}{m_t^2} (\bar{\xi}_{N,tt}^U + \bar{\xi}_{N,tc}^U \frac{V_{cs}^*}{V_{ts}^*}) (\bar{\xi}_{N,tt}^U + \bar{\xi}_{N,tc}^U \frac{V_{cb}}{V_{tb}}) G_1(y), \\ &+ \frac{1}{m_t m_b} (\bar{\xi}_{N,tt}^U + \bar{\xi}_{N,tc}^U \frac{V_{cs}^*}{V_{ts}^*}) (\bar{\xi}_{N,bb}^D + \bar{\xi}_{N,sb}^D \frac{V_{ts}}{V_{tb}}) G_2(y). \end{aligned} \quad (12)$$

For the second set of operators eq. (10) we get,

$$\begin{aligned} C_{1,\dots,6,9,10}'^{SM}(m_W) &= 0, \\ \end{aligned} \quad (13)$$

$$\begin{aligned} C_{1,\dots,6,9,10}'^H(m_W) &= 0, \\ C_7'^H(m_W) &= \frac{1}{m_t^2} (\bar{\xi}_{N,bs}^D \frac{V_{tb}}{V_{ts}^*} + \bar{\xi}_{N,ss}^D) (\bar{\xi}_{N,bb}^D + \bar{\xi}_{N,sb}^D \frac{V_{ts}}{V_{tb}}) F_1(y), \\ &+ \frac{1}{m_t m_b} (\bar{\xi}_{N,bs}^D \frac{V_{tb}}{V_{ts}^*} + \bar{\xi}_{N,ss}^D) (\bar{\xi}_{N,tt}^U + \bar{\xi}_{N,tc}^U \frac{V_{cb}}{V_{tb}}) F_2(y), \\ C_8'^H(m_W) &= \frac{1}{m_t^2} (\bar{\xi}_{N,bs}^D \frac{V_{tb}}{V_{ts}^*} + \bar{\xi}_{N,ss}^D) (\bar{\xi}_{N,bb}^D + \bar{\xi}_{N,sb}^D \frac{V_{ts}}{V_{tb}}) G_1(y), \end{aligned}$$

$$+ \frac{1}{m_t m_b} (\bar{\xi}_{N,bs}^D \frac{V_{tb}}{V_{ts}^*} + \bar{\xi}_{N,ss}^D) (\bar{\xi}_{N,tt}^U + \bar{\xi}_{N,tc}^U \frac{V_{cb}}{V_{tb}}) G_2(y) , \quad (14)$$

where $x = m_t^2/m_W^2$ and $y = m_t^2/m_{H^\pm}^2$. Here we used the redefinition

$$\xi^{U,D} = \frac{4G_F}{\sqrt{2}} \bar{\xi}^{U,D} . \quad (15)$$

The functions $F_1(y)$, $F_2(y)$, $G_1(y)$ and $G_2(y)$ are given as

$$\begin{aligned} F_1(y) &= \frac{y(7 - 5y - 8y^2)}{72(y-1)^3} + \frac{y^2(3y-2)}{12(y-1)^4} \ln y , \\ F_2(y) &= \frac{y(5y-3)}{12(y-1)^2} + \frac{y(-3y+2)}{6(y-1)^3} \ln y , \\ G_1(y) &= \frac{y(-y^2+5y+2)}{24(y-1)^3} + \frac{-y^2}{4(y-1)^4} \ln y , \\ G_2(y) &= \frac{y(y-3)}{4(y-1)^2} + \frac{y}{2(y-1)^3} \ln y . \end{aligned} \quad (16)$$

Note that we neglect the contributions of the internal u and c quarks compared to one due to the internal t quark.

For the initial values of the mentioned Wilson coefficients in the model III (eqs. (11), (12), (13) and (14), we have

$$\begin{aligned} C_{1,3,\dots,6,9,10}^{2HDM}(m_W) &= 0 , \\ C_2^{2HDM}(m_W) &= 1 , \\ C_7^{2HDM}(m_W) &= C_7^{SM}(m_W) + C_7^H(m_W) , \\ C_8^{2HDM}(m_W) &= C_8^{SM}(m_W) + C_8^H(m_W) , \end{aligned} \quad (17)$$

$$\begin{aligned} C_{1,\dots,6,9,10}^{\prime 2HDM}(m_W) &= 0 , \\ C_7^{\prime 2HDM}(m_W) &= C_7^{\prime SM}(m_W) + C_7^{\prime H}(m_W) , \\ C_8^{\prime 2HDM}(m_W) &= C_8^{\prime SM}(m_W) + C_8^{\prime H}(m_W) . \end{aligned} \quad (18)$$

At this stage it is possible to obtain the result for model II, in the approximation $\frac{m_s}{m_b} \sim 0$ and $\frac{m_b^2}{m_t^2} \sim 0$, by making the following replacements in the Wilson coefficients:

$$\begin{aligned} \bar{\xi}_{st}^{U*} \bar{\xi}_{tb}^U &= m_t^2 \frac{1}{\tan^2 \beta} , \\ \bar{\xi}_{st}^{U*} \bar{\xi}_{tb}^D &= -m_t m_b , \end{aligned} \quad (19)$$

and taking "0" for the coefficients due to the flipped operator set, i.e $C'_i \rightarrow 0$.

Using the initial values, we can calculate the coefficients C_i^{2HDM} and $C_i'^{2HDM}$ at any lower scale with five quark effective theory where large logarithms can be summed using the renormalization group. Since the strong interactions preserve chirality, the operators in eqs. (8, 9) can not mix with their chirality flipped counterparts eq. (10) and the anomalous dimension matrices of two separate set of operators are the same and do not overlap. With the above chosen initial values of Wilson coefficients, their evaluations are similar to the SM case.

Further, the operators O_5, O_6, O_9 and O_{10} (O'_5, O'_6, O'_9 and O'_{10}) give a contribution to the leading order matrix element of $b \rightarrow s\gamma$ and in the NDR scheme which we use here, the effective magnetic moment type Wilson coefficients are redefined as

$$\begin{aligned} C_7^{eff}(\mu) &= C_7^{2HDM}(\mu) + Q_d (C_5^{2HDM}(\mu) + N_c C_6^{2HDM}(\mu)) , \\ &+ Q_u \left(\frac{m_c}{m_b} C_{10}^{2HDM}(\mu) + N_c \frac{m_c}{m_b} C_9^{2HDM}(\mu) \right) , \\ C_7'^{eff}(\mu) &= C_7'^{2HDM}(\mu) + Q_d (C_5'^{2HDM}(\mu) + N_c C_6'^{2HDM}(\mu)) \\ &+ Q_u \left(\frac{m_c}{m_b} C_{10}'^{2HDM}(\mu) + N_c \frac{m_c}{m_b} C_9'^{2HDM}(\mu) \right) , \end{aligned}$$

where N_c is the color factor and Q_u (Q_d) is the charge of up (down) quarks. The LLog corrected coefficients $C_7^{2HDM}(\mu)$ and $C_7'^{2HDM}(\mu)$ are given as

$$\begin{aligned} C_7^{2HDM}(\mu) &= \eta^{16/23} C_7^{2HDM}(m_W) + (8/3)(\eta^{14/23} - \eta^{16/23}) C_8^{2HDM}(m_W) \\ &+ C_2^{2HDM}(m_W) \sum_{i=1}^8 h_i \eta^{a_i} , \\ C_7'^{2HDM}(\mu) &= \eta^{16/23} C_7'^{2HDM}(m_W) + (8/3)(\eta^{14/23} - \eta^{16/23}) C_8'^{2HDM}(m_W) . \end{aligned} \quad (20)$$

Here $\eta = \alpha_s(m_W)/\alpha_s(\mu)$. h_i and a_i are the numbers which appear during the evaluation [14]. The LLog corrected coefficients $C_5^{2HDM}(\mu)$, $C_6^{2HDM}(\mu)$ and $C_5'^{2HDM}(\mu)$, $C_6'^{2HDM}(\mu)$ are small numbers at m_b scale [12], which we neglect in our calculations.

There is still another mixing in the operator set O_7, O_8, O_9, O_{10} ($O'_7, O'_8, O'_9, O'_{10}$) [10] and we do not take into account since the initial values of the Wilson coefficients C_{10} and C'_{10} are zero in our case.

Finally, the LLog QCD corrected $b \rightarrow s\gamma$ decay rate in model III is obtained as

$$\Gamma(b \rightarrow s\gamma) = \frac{G_F^2 m_b^5}{32\pi^4} \alpha_{em} |V_{ts}^* V_{tb}|^2 (|C_7^{eff}(m_b)|^2 + |C_7'^{eff}(m_b)|^2) , \quad (21)$$

where α_{em} is the fine structure constant, and m_b is b-quark mass. $C_7^{eff}(m_b)$ and $C_7'^{eff}(m_b)$ are given in eq.(20) by choosing $\mu = m_b$.

3 Constraint analysis

Now let us turn our attention to the constraint analysis. Restrictions to the free parameters, namely, the masses of the charged and neutral Higgs bosons and the ratio of the v.e.v. of the two Higgs fields, denoted by $\tan\beta$ in the framework of model I and II, have been predicted in series of works [15]. Recently the constraint which connects masses of the charged Higgs bosons, m_{H^\pm} and $\tan\beta$, is obtained by using the QCD corrected values in the LLog approximation and it is shown that the constraint region is sensitive to the renormalization scale, μ [16].

The study of $R_b = \Gamma(Z \rightarrow b\bar{b})/\Gamma(Z \rightarrow \text{hadrons})$ ratio is a one of the possibility to derive the restrictions for the free parameters in the model III [6]. A considerable enhancement to the SM result is reached under the conditions $\xi_{bb}^D > \frac{60m_b}{v}$ and $m_{H^\pm} \sim 400 \text{ GeV}$, where ξ_{bb}^D is a model III parameter (see section 2) and v is the vacuum expectation value of the Higgs field responsible for the generation of fermion masses. Usually, the stronger restrictions to the new couplings are obtained from the analysis of $\Delta F = 2$ (here $F = K, B_d, D$) decays.

The constraints for the FC couplings from $\Delta F = 2$ processes for the model III was investigated without QCD corrections, under the following assumption [9]

1. $\lambda_{ij} \sim \lambda$,
2. $\lambda_{uj} = \lambda_{dj} \ll 1$, $i, j = 1, 2, 3$,

where i, j are the generation numbers.

3. case 2 and further assumption

$$\lambda_{bb}, \lambda_{sb} \gg 1 \text{ and } \lambda_{tt}, \lambda_{ct} \ll 1 . \quad (22)$$

In the analysis, the ansatz

$$\xi_{ij}^{UD} = \lambda_{ij} \sqrt{\frac{m_i m_j}{v}} , \quad (23)$$

is used. Note that it coincides with the one proposed by Cheng and Sher.

Using the constraint from R_b^{exp} , the measurement $Br(B \rightarrow X_s \gamma)$, ΔF mixing and the result due to ρ parameter, the following restrictions are predicted [9]

$$\begin{aligned} 150 \text{ GeV} &\leq m_{H^\pm} \leq 200 \text{ GeV} , \\ \lambda_{bb} &\gg 1 , \lambda_{tt} \ll 1 , \\ \lambda_{sb} &\gg 1 , \lambda_{ct} \ll 1 . \end{aligned} \quad (24)$$

In the present work, we analyse the restrictions for the couplings $\bar{\xi}_{Ntt}^U$, $\bar{\xi}_{Nb}^D$ and $\bar{\xi}_{Ntc}^U$ in the LLog approximation using the prediction from R_b^{exp} , namely $\xi_{bb}^D > \frac{60m_b}{v}$, and the measurement by the CLEO collaboration [2]:

$$Br(B \rightarrow X_s \gamma) = (2.32 \pm 0.57 \pm 0.35) \cdot 10^{-4}. \quad (25)$$

The idea in this calculation is to take $\bar{\xi}_{Ntc} << \bar{\xi}_{Ntt}^U, \bar{\xi}_{Nb}^D$ and $\bar{\xi}_{Nsb}^D \sim 0, \bar{\xi}_{Nss}^D \sim 0$. This choice gives a simplification since the Wilson coefficient C'_7 can be neglected. Further the neutral Higgs contributions are also suppressed because the Yukawa vertices are the combinations of $\bar{\xi}_{Nsb}^D$ and $\bar{\xi}_{Nss}^D$.

To reduce the b-quark mass dependence let us consider the ratio

$$\begin{aligned} R &= \frac{Br(B \rightarrow X_s \gamma)}{Br(B \rightarrow X_c e \bar{\nu}_e)} \\ &= \frac{|V_{ts}^* V_{tb}|^2}{|V_{cb}|^2} \frac{6\alpha_{em}}{\pi g(z) \kappa(z)} |C_7^{eff}|^2, \end{aligned} \quad (26)$$

where $g(z)$ is the phase space factor in semileptonic b-decay, $\kappa(z)$ is the QCD correction to the semileptonic decay width [17],

$$\begin{aligned} g(z) &= 1 - 8z^2 + 8z^6 + z^8 - 24z^4 \ln z, \\ \kappa(z) &= 1 - \frac{2\alpha_s(m_b)}{3\pi} \left\{ \left(\pi^2 - \frac{31}{4} \right) (1-z) + \frac{3}{2} \right\}, \end{aligned} \quad (27)$$

and $z = m_c/m_b$.

Following the same procedure used in [16], we reach the possible range for $|C_7^{eff}|$ as

$$0.1930 \leq |C_7^{eff}| \leq 0.4049. \quad (28)$$

In fig. (1) (fig. (2)), we plot the parameter $\bar{\xi}_{N,tt}^U$ with respect to $\bar{\xi}_{N,bb}^D$ for fixed μ scale $\mu = 2.5 \text{ GeV}$ and mass of the charged Higgs boson $m_{H^\pm} = 400 \text{ GeV}$ ($m_{H^\pm} = 800 \text{ GeV}$). We see, that there are two different restriction regions, where the upper one corresponds to the positive C_7^{eff} value, however the lower one to the negative C_7^{eff} value. Increasing $\bar{\xi}_{N,bb}^D$ causes $|\bar{\xi}_{N,tt}^U|$ to decrease in both regions. With the given restriction $\xi_{bb}^D > \frac{60m_b}{v}$, the condition $|r_{tb}| = \left| \frac{\bar{\xi}_{N,tt}^U}{\bar{\xi}_{N,bb}^D} \right| < 1$ is obtained. In the lower region it is possible that the ratio becomes negative, i.e. $r_{tb} = \frac{\bar{\xi}_{N,tt}^U}{\bar{\xi}_{N,bb}^D} < 0$. Further $|r_{tb}|$ increases with increasing m_{H^\pm} .

Fig. (3) (fig. (4)) shows the same dependence for fixed μ scale, $\mu = 5 \text{ GeV}$ ($m_W \text{ GeV}$) and $m_{H^\pm} = 400 \text{ GeV}$. It is shown that the ratio r_{tb} is sensitive to the renormalization scale and becomes larger in the upper region with decreasing μ . However, in the lower region the restricted area for negative ratios ($r_{tb} < 0$) becomes small.

Fig. (5) (figs. (6) and (7)) is devoted the same dependence as in fig. (1) (figs. (2) and (3)) and shows that the third region, which is almost a straight line, appears. In this region the ratio $r_{tb} \gg 1$ and increases with increasing m_{H^\pm} similar to the previous regions. In addition, it is non-sensitive to LLog QCD corrections.

In Fig. (8) and fig. (10) ((fig. (9) and fig. (11)) we present the dependence of $\bar{\xi}_{N,tt}^U$ to m_{H^\pm} for fixed $\bar{\xi}_{N,bb}^D = 60 m_b$ ($\bar{\xi}_{N,bb}^D = 80 m_b$) and at the scale $\mu = 2.5 \text{ GeV}$. The strong m_{H^\pm} dependence of $\bar{\xi}_{N,tt}^U$ is realized in the three different regions, which one is almost a curve fig. (10) (fig. (11)) and represents $r_{tb} \gg 1$.

Finally, we consider $\bar{\xi}_{N,tt}^U$ dependence of $\bar{\xi}_{N,tc}^U$, which is a neutral FC coupling. In Fig. (12) (fig. (13)) we plot the $\bar{\xi}_{N,tt}^U$ dependence of $\bar{\xi}_{N,tc}^U$ for fixed $\bar{\xi}_{N,bb}^D = 60 m_b$, at the scale $\mu = 2.5 \text{ GeV}$, and charged Higgs mass $m_{H^\pm} = 400 \text{ GeV}$ ($m_{H^\pm} = 800 \text{ GeV}$). Here the selected region for $\bar{\xi}_{N,tt}^U$ is $24 \leq \bar{\xi}_{N,tt}^U \leq 36$ ($56 \leq \bar{\xi}_{N,tt}^U \leq 76$). Increasing $\bar{\xi}_{N,tt}^U$ forces the ratio $r_{tc} = \frac{\bar{\xi}_{N,tc}^U}{\bar{\xi}_{N,tt}^U}$ to be negative. It is realized that the ratio $|r_{tc}|$ becomes smaller when m_{H^\pm} is larger. Still there is a region in which $\bar{\xi}_{N,tc}^U$ is constrained for the possible large value of $\bar{\xi}_{N,tt}^U$, namely $\bar{\xi}_{N,tt}^U = 84 \cdot 10^3$. This region is estimated for $m_{H^\pm} = 400 \text{ GeV}$ as

$$\begin{aligned} 0.97 < \bar{\xi}_{N,tc}^U < 1.35, \text{ or} \\ -0.09 < \bar{\xi}_{N,tc}^U < 0.284, \end{aligned} \quad (29)$$

and for $m_{H^\pm} = 800 \text{ GeV}$ as

$$\begin{aligned} 2.12 < \bar{\xi}_{N,tc}^U < 3.07, \text{ or} \\ -0.21 < \bar{\xi}_{N,tc}^U < 0.645. \end{aligned} \quad (30)$$

In Fig. (14) we present the same dependence for the scale $\mu = 5 \text{ GeV}$ and we see that increasing μ scale decreases the ratio $|r_{tc}|$. Another possible region for $\bar{\xi}_{N,tc}^U$ in the case $\bar{\xi}_{N,tc}^U = 84 \cdot 10^3$ and $m_{H^\pm} = 400 \text{ GeV}$ is

$$\begin{aligned} 0.81 < \bar{\xi}_{N,tc}^U < 1.15, \text{ or} \\ -0.15 < \bar{\xi}_{N,tc}^U < 0.188, \end{aligned} \quad (31)$$

In conclusion, we predicted the constraints for the Yukawa couplings $\bar{\xi}_{N,tt}^U$, $\bar{\xi}_{N,bb}^D$ and $\bar{\xi}_{N,tc}^U$ using the CLEO measurement $Br(B \rightarrow X_s \gamma)$ and the lower bound of $\bar{\xi}_{N,bb}^D$ from the experimental result of R_b value. In the calculations we have neglected the neutral Higgs boson contributions, since we assume that $\bar{\xi}_{N,bs}^D$, $\bar{\xi}_{N,ss}^D$ and $\bar{\xi}_{N,cc}^U$ are small enough.

The uncertainty due to QCD corrections in the leading order is signalled by the dependence on the renormalization scale μ . With the choice $\mu = \frac{m_b}{2}$ ($\sim 2.5 \text{ GeV}$), the LLog approximation

reproduce effectively the NLO result. The constraints for the other parameters of the model III from the existing experimental results require more detailed and comprehensive analysis.

References

- [1] J. L. Hewett, in proc. of the 21st Annual SLAC Summer Institute, ed. L. De Porcel and C. Dunwoode, SLAC-PUB6521.
- [2] M. S. Alam et al., CLEO Collaboration, Phys. Rev. Lett. **74** (1995) 2885.
- [3] R. Ammar et al., CLEO Collaboration, Phys. Rev. Lett **71** (1993) 674.
- [4] S. L. Glashow and S. Weinberg, Phys. Rev. D**15** (1977) 1958.
- [5] H. Haber, C. Kane, and T. Sterlig, Nucl. Phys. Lett.B **161** (1979) 493;
- [6] D. Atwood, L. Reina and A. Soni, Phys. Rev. D**53** (1996) 119.
- [7] D. Atwood, L. Reina and A. Soni, Phys. Rev. Lett. **75** (1995) 3800.
- [8] T. P. Cheng and M. Sher, Phys. Rev. D **35** (1987) 3484; Phys. Rev. D **44** (1991) 1461; A. Antaramian, L. J. Hall and A. Rasin, Phys. Rev. Lett. **69** (1992) 1871; L. J. Hall and S. Weinberg, Phys. Rev. D **48** (1993) 979; M. Savage, Phys. Lett. B **266** (1991) 135; M. Luke and M. G. Savage, Phys. Lett. B**307** (1993) 387.
- [9] D. Atwood, L. Reina and A. Soni, Phys. Rev. D **55** (1997) 3156.
- [10] P. Cho and Misiak, Phys. Rev. D**49** (1994) 5894.
- [11] M. Misiak, Phys. B**269** (1991) 161.
- [12] G. Hiller and E. Iltan, Phys. Lett B **409** (1997) 425.
- [13] A. Ali and C. Greub, Z. Phys. C **49** (1991) 431; A. J. Buras et al., Nucl. Phys. B **424** (1994) 374.
- [14] A. J. Buras, M. Misiak, M. Münz and S. Pokorski, Nucl. Phys. B**424** (1994) 374.

[15] P. Abreu et al., *Z. Phys. C* **64** (1994) 183;
 G. Alexander et al., *Phys. Lett. B* **370** (1996) 17;
 M. Veltman, *Acta Phys. Polon. B* **8** (1977) 475;
 B. W. Lee, C. Quigg, H. B. Thacker, *Phys. Rev. D* **16** (1977) 253;
 M. Veltman, *Phys. Lett. B* **70** (1977) 253;
 F. Abe et al., hep-ex/9704003. A. K. Grant, *Phys. Rev. D* **51** (1995) 207;
 M. Acciari et al., *Phys. Lett. D* **396** (1997) 327;
 ALEPH Collaboration, contributed to ICHEP, Warsaw, Poland, 25-31, July 1996, Pr. No: PA10-019;
 K. Kiers and A. Soni, *Phys. Rev D* **56** (1997) 5786.

[16] T. M. Aliev, G. Hiller and E. O. Iltan, hep-ph/9708382

[17] N. Cabibbo and L. Mainani, *Phys. Lett. B* **79** (1978) 109

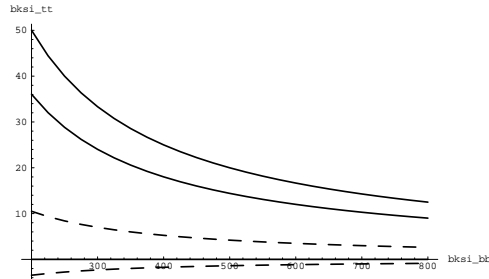


Figure 1: $\bar{\xi}_{Ntt}^U$ as a function of $\bar{\xi}_{Nbb}^D$ for the fixed value of the charged Higgs boson mass $m_{H^\pm} = 400\text{ GeV}$ at the scale $\mu = 2.5\text{ GeV}$. Here the constraint region is lying in between solid (dashed) curves. The solid (dashed) curves are the boundaries of the constraint region corresponding to $C_7^{eff} > 0$ ($C_7^{eff} < 0$)

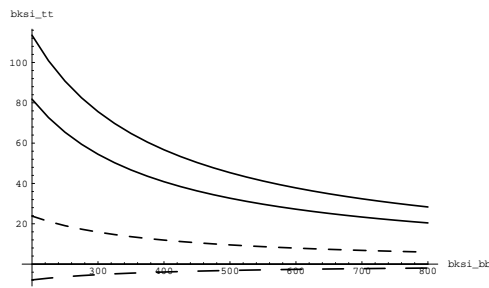


Figure 2: Same as fig 1 but for $m_{H^\pm} = 800 \text{ GeV}$.

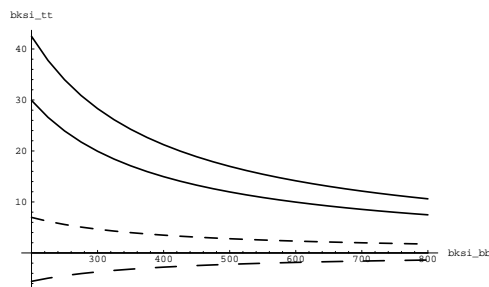


Figure 3: Same as fig 1 but at $\mu = 5 \text{ GeV}$.

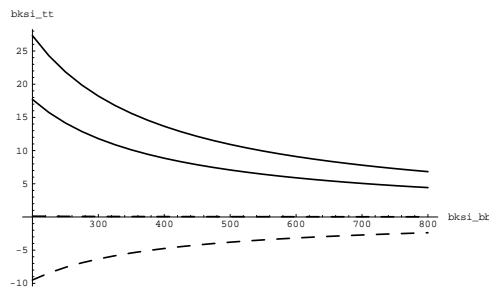


Figure 4: Same as fig 1 but at $\mu = m_W \text{ GeV}$.

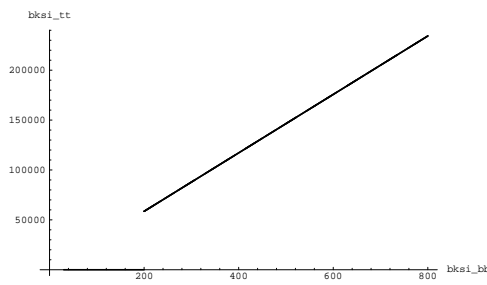


Figure 5: Same as fig 1, but the third possible constraint region.

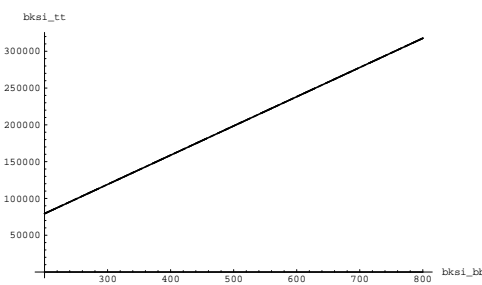


Figure 6: Same as fig 2, but the third possible constraint region.

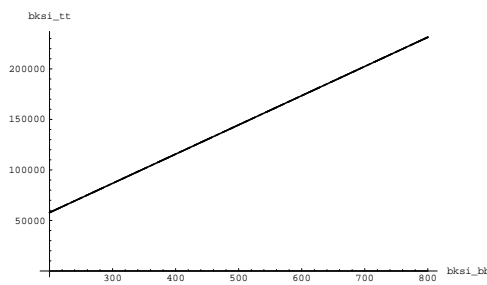


Figure 7: Same as fig 3, but the third possible constraint region.

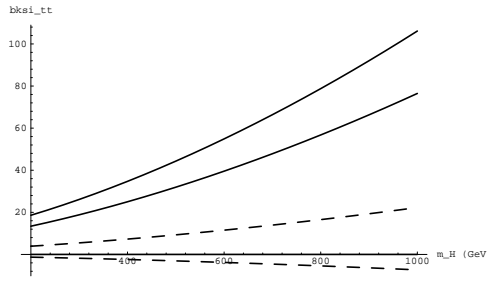


Figure 8: m_{H^\pm} dependence of $\bar{\xi}_{Ntt}^U$ for the fixed $\bar{\xi}_{Nbb}^U = 60 m_b$ and the scale $\mu = 2.5 \text{ GeV}$ Here the constraint region is lying in between solid curves (dashed curves). The solid (dashed) curves are the boundaries of the constraint region corresponding to $C_7^{eff} > 0$ ($C_7^{eff} < 0$)

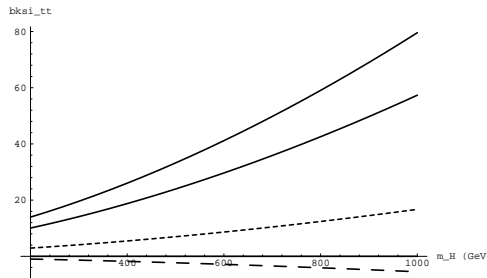


Figure 9: Same as fig 8, but for $\bar{\xi}_{Nbb}^U = 80 m_b$.

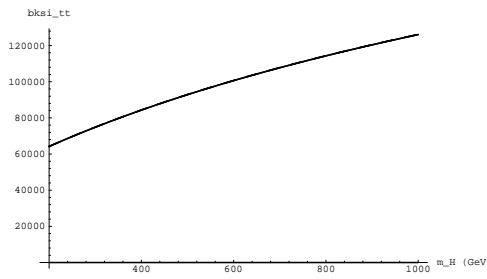


Figure 10: Same as fig 8 but the third possible constraint region.

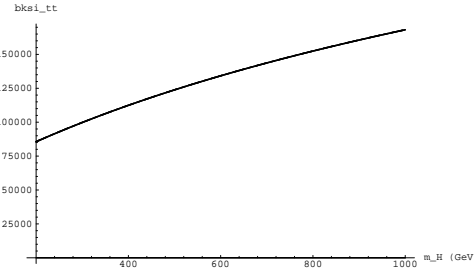


Figure 11: Same as fig 9, but the third possible constraint region.

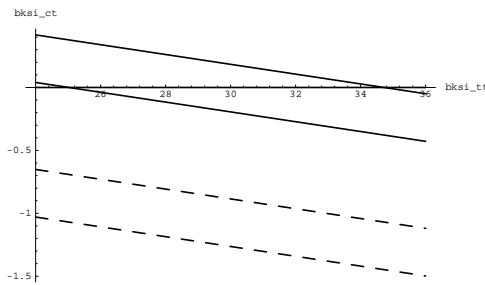


Figure 12: $\bar{\xi}_{Ntt}^U$ dependence of $\bar{\xi}_{Nct}^U$ for the fixed $\bar{\xi}_{Nbb}^U = 60 m_b$, the scale $\mu = 2.5 \text{ GeV}$ and $m_{H^\pm} = 400 \text{ GeV}$. Here the constraint region is lying in between solid curves (dashed curves). The solid (dashed) curves are the boundaries of the constraint region corresponding to $C_7^{eff} > 0$ ($C_7^{eff} < 0$)

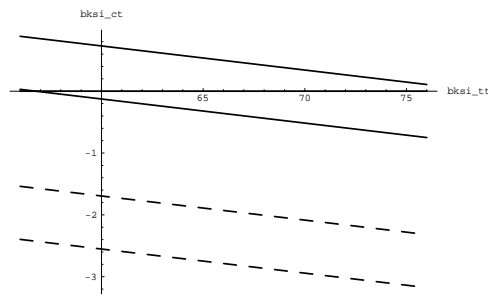


Figure 13: Same as fig 12, but for $m_{H^\pm} = 800 \text{ GeV}$.

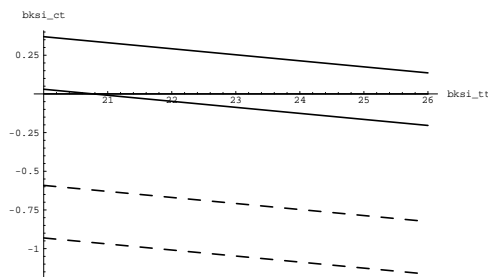


Figure 14: Same as fig 12, but at $\mu = 5 \text{ GeV}$.